Catalysis Today 175 (2011) 147–156

Contents lists available at ScienceDirect

Catalysis Today

journal homepage: www.elsevier.com/locate/cattod

Review

# Low-temperature selective catalytic reduction of $NO_x$ with $NH_3$ over metal oxide and zeolite catalysts—A review

Junhua Li[a,b,*], Huazhen Chang[a], Lei Ma[a], Jiming Hao[a], Ralph T. Yang[b]

[a] *Department of Environmental Science and Engineering, Tsinghua University, Beijing 100084, People's Republic of China*
[b] *Department of Chemical Engineering, University of Michigan, Ann Arbor, MI 48109, USA*

ARTICLE INFO

*Article history:*
Received 31 October 2010
Received in revised form 20 February 2011
Accepted 14 March 2011
Available online 13 April 2011

*Key words:*
SCR of $NO_x$ with ammonia
Metal oxide catalysts
$MnO_2$
Cu, Fe-exchanged zeolites
Fe-beta
Reaction mechanism

ABSTRACT

The removal of $NO_x$ by catalytic technology at low temperatures (100–300 °C) is significant for flue gas of industry and exhaust gas of diesel engine; however, to develop the low-temperature catalyst (LTC) for selective catalytic reduction of $NO_x$ with ammonia ($NH_3$-SCR) is still a challenge especially at temperature below 200 °C. This study reviews two types of LTC, the metal oxide catalyst and metal exchanged zeolite catalyst. The performances of Mn-based metal oxide with and without supports have been attempted to correlate with preparation method, precursor, and various supports. The role of manganese oxides with different phases as the most effective low temperature active component and the limitation of stability in the presence of $H_2O$ and $SO_2$ are discussed. Fe, Cu exchanged zeolites as potential real application catalysts in diesel engine have been investigated for $NH_3$-SCR of $NO_x$ in the past decades, the activity, selectivity and thermal stability related to types of metal, and zeolite, and reaction conditions are reviewed. The research progress in active sites and reaction mechanisms of Mn-based catalyst and Fe–zeolite catalysts are described and compared. Finally, future research directions in the developing LTC for removal of $NO_x$ are proposed.

**Contents**

## 1. Introduction

Nitrogen oxides ($NO_x$, $x = 1{,}2$), as major air pollutants, are resulting in a series of environmental issues, such as photochemical smog, acid rain, ozone depletion, and fine particle pollution. It is well known that 90% of $NO_x$ emission inventory comes from com-

---

* Corresponding author at: Department of Environmental Science and Engineering, Tsinghua University, Beijing 100084, People's Republic of China.
Tel.: +86 10 62771093; fax: +86 10 62771093.
*E-mail address:* lijunhua@tsinghua.edu.cn (J. Li).

0920-5861/$ – see front matter © 2011 Elsevier B.V. All rights reserved.
doi:10.1016/j.cattod.2011.03.034

bustion, including the stationary source and mobile source. In fuel combustion from stationary sources, $NO_x$ are primarily from power stations, industrial heaters, and cogeneration plants [1,2]. The $NO_x$ emission from mobile source is mainly from the exhaust gas of gasoline and diesel engines. Due to the harmful and multi environmental impacts on the atmosphere, $NO_x$ emission legislation is becoming more and more stringent both for mobile and stationary sources. In capital of China, Beijing, $NO_x$ emission limits are $100\,mg\,m^{-3}$ for the case of power plants and $150\,mg\,m^{-3}$ for the case of gas, oil, and coal-fired industrial boiler (DB11/139-2007). The cut points of $NO_x$ in Chinese National 4 standards for automobile emission control are lower than 10% of that in Chinese National 0 standards.

To meet the stringent regulation, many efforts have been made to reduce $NO_x$ emission by using advanced combustion technologies or by using post-combustion abatement technologies. Regarding stationary sources, about 30–50% reduction in $NO_x$ emission can be achieved through advanced combustion technologies, and $NO_x$ removal technologies for flue gas are then taken to diminish the remaining $NO_x$ to meet the stringent environmental regulations. For mobile sources, although $NO_x$ from gasoline is very efficiently reduced by means of a three-way catalyst (TWC), this technology cannot be applied in the lean burn gasoline and diesel engines. In both flue gas of power plants and exhaust gas of vehicles, the typical features are the presence of excess oxygen, water vapor, and $SO_2$ in real operating conditions. Among various kinds of $NO_x$ removal technologies, NO direct thermal decomposition to $N_2$ and $O_2$ is an ideal way, however, this reaction is kinetically very difficult to achieve in the presence of oxygen, and up to date no catalyst has been successfully developed to the real application in a vehicle. $NH_3$-SCR of $NO_x$ is considered to be the most efficient and widely used technology for reducing $NO_x$ emissions from stationary sources [3,4]. It is now a mature technology that has been employed in diesel vehicles as well with urea as reductant [5].

The reaction equation for ammonia is given by:

$$2NO + 2NH_3 + (1/2)O_2 \rightarrow 2N_2 + 3H_2O$$

The reaction for urea is given by:

$$2NO + CO(NH_2)_2 + (1/2)O_2 \rightarrow 2N_2 + CO_2 + 2H_2O$$

Basically, the catalyst is crucial to the SCR of $NO_x$ with ammonia or urea technology. Nowadays, the commercial catalysts used for SCR in industry are based mainly on $TiO_2$-supported $V_2O_5$, promoted with $WO_3$, and a relative high conversion only at 350–400 °C is achieved on $V_2O_5$–$WO_3$/$TiO_2$ [3]. This type of catalyst has also been used for HD diesel vehicles in Europe. Although catalysts of vanadium have been introduced into the market for power plants and diesel vehicles, some problems still remain due to the high activity for oxidation of $SO_2$ to $SO_3$, the rapid decrease in activity and selectivity above 550 °C, and the toxicity of the vanadium species to the eco environment [6–8]. Moreover, the $V_2O_5$–$WO_3$/$TiO_2$ catalyst used for industry has to be installed upstream the particulate collector and flue gas desulfurization in order to meet the optimum working temperature of 350–400 °C. This type commercial catalyst is not available in the diesel engine as it cannot completely remove $NO_x$ due to the wide temperature window of exhaust gas (150–500 °C). Therefore, researchers in the field of academia and industry continue to develop new LTC that can work well around 250 °C or even below, in which the SCR unit could be placed behind the electric precipitation and desulfurizer in power plant and efficiently remove $NO_x$ at wider temperature range for $NO_x$ control in diesel engine. Up to date, many studies have been devoted to the development of traditional SCR technology [1,3,9,10]. Many aspects of either detailed reaction mechanisms or material properties of different catalyst systems were reported, however, only very limited efforts have been made to summarize the development and limitations of low temperature SCR catalysts.

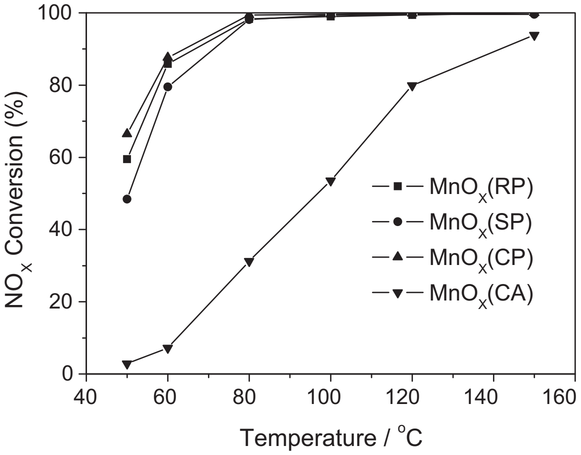

**Fig. 1.** $NO_x$ conversion as function of temperature over $MnO_x$ catalysts prepared with various methods. Reaction conditions: 0.5 g samples, 500 ppm NO, 500 ppm $NH_3$, 3% $O_2$, $N_2$ to balance, GHSV = 47,000 $h^{-1}$ [15].

In this paper, the research progress on $NH_3$-SCR of $NO_x$ at low temperatures is reviewed over the metal oxide and metal exchanged zeolite catalysts. We focus on the SCR performances over Mn-based metal oxide, and Fe, Cu exchanged zeolite catalysts. The aspects of possible mechanism and restricting of the application of low temperature SCR are discussed.

## 2. Low-temperature SCR catalysts

Up to now, LTC has been studied using $V_2O_5$, $Fe_2O_3$, and $MnO_x$ as the active components. Taking into consideration that the influence of components and environmental temperature to the formation of $(NH_4)_2SO_4$, $NH_4NO_3$ and $N_2O$ in flue gas, the main goal of the research is to utilize new carrier and develop low-temperature SCR catalysts with good activity, high selectivity, high stability and broad range of operating temperature. Such a catalyst would be placed downstream the electrostatic precipitator and even downstream desulfurizer, and the temperature at this point is lower than 160 °C. However, this type of LTC has never been demonstrated on the removal of $NO_x$ in flue gas of power plant.

### 2.1. Single metal oxide catalyst ($MnO_x$)

According to literatures, many SCR catalysts containing transitional metal (Fe, V, Cr, Cu, Co and Mn) have good low-temperature SCR activity [11–14]. Among them, the nano-$MnO_x$ catalyst has been studied extensively because of its excellent low temperature performance.

The crystallinity is dependent on the preparation methods and calcination temperature. Tang et al. [15] prepared manganese oxide catalysts by rheological phase reaction (RP), low temperature solid phase reaction (SP), co-precipitation (CP) and citric acid method (CA). The results showed that $Mn_2O_3$ formed by citric acid method is highly crystalline, while part of $MnO_x$ (RP) calcinated at 350 °C, and $MnO_x$ obtained by SP and CP method transformed into an amorphous phase. Fig. 1 shows the $NO_x$ conversion as function of temperature over unsupported $MnO_x$ catalysts prepared by various methods [15]. It shows $MnO_x$ with lower crystallinity exhibited higher activity at low temperature. Kang et al. [16,17] prepared manganese oxide catalysts by a precipitation method and investigated the effects of precipitant and calcination temperature. It was reported that the catalyst precipitated by sodium carbonate ($MnO_x$–SC) had the higher surface area than others, which may contribute to its first-rate performance. Besides, the partial decomposition and amorphous structure of the $MnO_x$–SC catalyst may also be a reason for the relatively higher activity.

The crystallinity, specific surface area, and oxidation state of $MnO_x$ are all correlated to the performance to some extent. Amorphous structure, which possesses huge surface area, is favorable for low temperature SCR. Several kinds of manganese oxides are known, for example, $MnO_2$, $Mn_5O_8$, $Mn_2O_3$, $Mn_3O_4$, and MnO, which are all stable in ambient conditions. Kapteijn et al. [18] reported that $MnO_2$ exhibited the highest low temperature activity per unit surface area and $Mn_2O_3$ with the highest $N_2$ selectivity. The onset temperature of reduction in TPR was: $MnO_2(C) < Mn_5O_8 < Mn_2O_3(C) < Mn_3O_4(C)$, which was correlated with the activity. The selectivity of $N_2$ decreased with increasing temperature over all kinds of $MnO_x$. At the same temperature, the decrease of $N_2$ selectivity with increasing NO conversion suggested that the partial pressure of reactants affected the products and a series of reaction mechanisms maybe involved at the catalyst surface. One possible way was that $NH_3$ could be oxidized to nitrous oxide and nitric oxide above 425 K over $MnO_x$. Tang et al. [19] reported the rates of both NO conversion and $N_2O$ formation per unit surface area on β-$MnO_2$ were much higher than the corresponding values on α-$Mn_2O_3$ (see Fig. 2). Higher selectivity of $N_2O$ was caused by lower Mn–O bond energy of β-$MnO_2$ which facilitated the activation of $NH_3$.

However, one problem in the studies of kinetic and mechanism on $MnO_x$ catalyst is the determination of the oxidation states and the amounts of the different phases and species of Mn, owing to the overlap of energy ranges for the various oxidation states of manganese. Galakhov et al. [20] suggested to determine the average oxidation state (AOS) of manganese based on a correlation between the binding energies of the doublet separation of Mn3s ($\Delta$Es) and the AOS. This method helps distinguish different oxidation states of Mn and has been widely used by researchers.

Moreover, it has been found that bimetallic and composite oxide catalysts containing Mn are both more active and more selective than $MnO_x$ [13,21–24]. It was reported that nearly 100% $N_2$ selectivity was obtained on $MnO_x$–$CeO_2$ at 100–150 °C [22], but the selectivity was relatively low on $MnO_x$ in this temperature range [15,19]. Kapteijn et al. [18] suggested that the activity and $N_2$ selectivity of the manganese oxide were determined by the oxidation state and the degree of crystallinity. Higher activated capability to $NH_3$, and more N–H bonds in $NH_3$ molecules broken on β-$MnO_2$ may contribute to higher $N_2O$ selectivity over β-$MnO_2$ [19].

## 2.2. *Multi-metal oxide catalysts*

### 2.2.1. *Composite oxide catalysts*

Composite oxide catalysts are of great interest because one metal element can modify the catalytic properties of another, which results from both electronic and structural influences. For example, binary metal oxide solid solutions might be formed between Mn and Cu, Ce, etc. [21–23]. In the composite oxide catalysts containing Mn, the molar ratio of Mn and doped metal is very important to the structure and dispersion of Mn. The oxidation state of Mn, which will affect the SCR activity of Mn-based composite oxide catalyst, would alter along with the changing of molar ratio of Mn [24]. Amorphous structure is considered to favor the low temperature SCR.

Mn-based bimetallic oxide catalysts show unusual performance in low temperature SCR. Long et al. [13] considered the superior SCR activity on Fe–Mn catalysts due to their high activity for NO oxidation to $NO_2$ at low temperatures. Qi et al. [22,23] investigated the low temperature SCR behavior of $MnO_x$–$CeO_2$ and found that the Mn/(Mn + Ce) molar ratio, calcination temperature and $O_2$ concentration would affect the performance significantly. The reaction on this catalyst was suggested to be zero order with respect to $NH_3$ and first order with respect to NO. Many other transition metals were doped to improve the performance of $MnO_x$–$CeO_2$. It was found that Fe and Zr modification increased the low temperature activity and $N_2$ selectivity, Pr could enhance the $N_2$ selectivity and resistance to $H_2O$ and $SO_2$ [22].

The calcination temperature affects the crystallinity and catalyst structure obviously. It was reported [25] with an increase in calcination temperature of iron titanate catalyst, particle size increased quickly along with the BET surface area decreasing rapidly. Liu et al. [26,27] investigated the manganese substituted iron titanate catalysts, which were prepared by co-precipitation method. The addition of Mn led to increasing of surface area and porosity, distortion and appropriate disorder of structure, enhancement of lattice oxygen mobility and $NO_x$ adsorption capacity.

At present, the effects of doped metals on electronic dispersion and crystal structure of Mn are not very clear yet. It needs to be further investigated. Besides, the improvement of $N_2$ selectivity and sulfur resistance of composite oxide catalysts will become one of the most important research targets in the future.

### 2.2.2. *Supported metal oxide catalysts*

For supported metal oxide catalysts, the active components mainly exist on the surface of the catalysts. The major roles of the supporters are: (a) providing huge surface to separate the active phase and prevent from the formation of big crystalline particles; (b) supplying the space where the catalytic reactions take place. Most supported metal oxide catalysts are prepared by impregnation method [28–33].

Many support materials, such as $A1_2O_3$ and $TiO_2$, have been investigated for low temperature SCR reaction. Chen et al. [32] studied alumina-supported transition metal sulfates as the low temperature $DeNO_x$ catalysts. The results showed that a $10\%NiSO_4/A1_2O_3$ catalyst exhibited $NO_x$ conversion of over 50% at 50–120 °C and nearly 80% $NO_x$ conversion at 200–250 °C under commercial SCR throughput and gas composition conditions. The author attributed the activity to the surface Brönsted acidity. Moreno-Tost et al. [31] investigated cobalt–iridium supported on zirconium-doped mesoporous silica as catalysts for $NH_3$-SCR and found that Co–Ir supported catalysts showed higher NO conversion and lower yield of $N_2O$ than Co supported catalyst. The enhancement of activity was due to increasing of the dispersion of cobalt and restricting of the formation of the cobalt spinel during the calcination process with Ir. The formation of $N_2O$ is still a problem in $V_2O_5$ containing catalysts. It was proposed the $N_2O$ generation over $V_2O_5/TiO_2$ catalysts at low temperature was due to the formation of surface V-ON species that came from the partial oxidation of adsorbed ammonia species with NO + $O_2$ (eventually $NO_2$). $N_2O$ molecule formed when these active sites were close enough. So the highly active site density caused by increasing in vanadium loading would enhance the formation of $N_2O$ [34].

$MnO_x/TiO_2$ catalyst has been investigated by some researchers. Li et al. [33] investigated the effect of precursors on the surface Mn species and the activities over $MnO_x/TiO_2$ catalysts. Catalysts prepared from manganese nitrate (MN) and manganese acetate (MA) showed different oxidation states and surface Mn atom concentrations. Crystal $MnO_2$ and some amount of Mn-nitrate were found in MN–$MnO_x/TiO_2$ sample, and highly dispersed surface $Mn_2O_3$ which was probably amorphous was found in MA–$MnO_x/TiO_2$. The SCR activity of the latter was much higher than the former at temperature below 200 °C. When cerium was doped in $MnO_x/TiO_2$, the chemisorbed oxygen concentration increased, which improved NO oxidation on catalyst surface. Meanwhile, the oxygen storage capacity of the catalyst and surface acidity were enhanced after modification. All of these factors promoted the activity in $NH_3$-SCR at low temperatures [35].

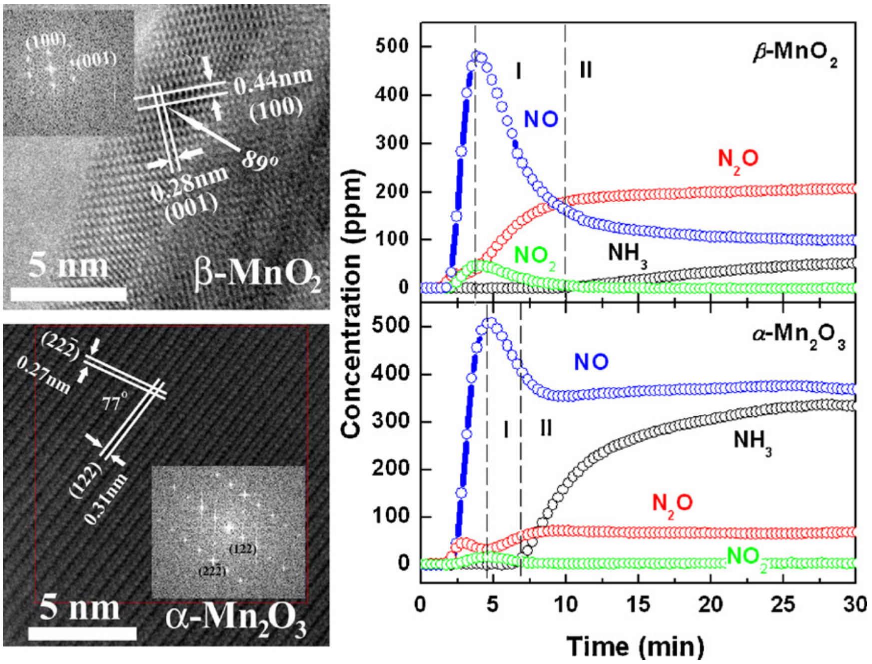

**Fig. 2.** TEM and transition reactions of $NH_3$ + NO on the catalysts in the presence of $O_2$. Reaction conditions: 0.2 g catalyst, 680 ppm NO, 680 ppm $NH_3$, 3.0% $O_2$, and $N_2$ balance, gas flow rate = 300 mL min$^{-1}$, temperature = 150 °C [19].

Casapu et al. [36] investigated the $NH_3$-SCR performance of $MnO_x$–$CeO_2$/cordierite catalysts and found that the activity of $NH_3$ oxidation on $MnO_x$–$CeO_2$–$Nb_2O_5$/cordierite was slightly higher than that of $MnO_x$–$CeO_2$/cordierite. The SCR performance below 200 °C was promoted on $Nb_2O_5$ doping sample compared with $MnO_x$–$CeO_2$/cordierite. The $NO_x$ conversion on $Nb_2O_5$ doping sample would be further improved by adding $NO_2$ to inlet gas, but $NH_4NO_3$ formation below 200 °C and $N_2O$ formation at higher temperatures restrained the application of this catalyst. Fig. 3 shows the $NO_x$ conversion on $MnO_x$–$CeO_2$–$Nb_2O_5$/cordierite catalyst with 10 ppm $NH_3$ slip [36].

However, the obstacle of the application of Mn-based catalysts is the poor performance of resisting $H_2O$ and $SO_2$. If composition can be changed to improve $H_2O$ and $SO_2$ resistance, catalysts with Mn could be widely used in the future. Catalyst with other active component, such as CuO [37], has also been studied.

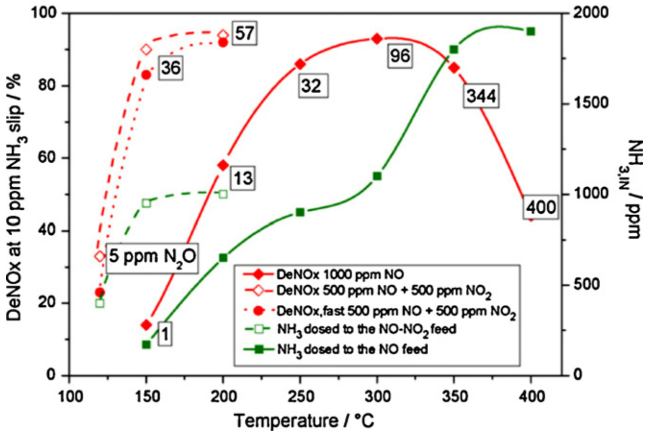

**Fig. 3.** $DeNO_x$ at a 10 ppm $NH_3$ slip vs. temperature of $MnO_x$–$CeO_2$–$Nb_2O_5$/cordierite catalyst. The "$DeNO_x$, fast" which is due to the fast SCR reaction is also shown. The amount of the ammonia dosed to the NO–$NO_2$ or to the NO feed is additionally displayed [36].

In the early 1970s, noble metal catalysts had been developed as emission control catalysts, on which Pt, Rh and Pd were employed as their active components and aluminum oxide or monolithic ceramics were as their supports [38]. As the earliest used catalysts, their characters were lower operating temperature and higher activity, but they also had disadvantages like oxidation of $NH_3$, sensitivity to $SO_2$, and high cost [39].

### 2.3. *Metal oxides supported on carbon materials*

In order to gain high surface area and pore structure, activated carbon becomes a good solid sorbent, and it is widely used in clarification of air or industry waste gas. To remove $NO_x$, it can be used not only as sorbent, but also as support of catalyst. Activated carbon is valuable for $NO_x$ removal in stationary source because it is of abundant resource, low price, and easy regeneration. However, the catalytic activity is low when activated carbon used as catalyst, especially in high space velocity conditions. It usually needs to be treated by pre-activation or loading of some active components to improve catalytic performance.

The methods of introducing the metals, concentration of the precursor solutions, the final drying methods (conventional or microwaves assisted), and contact time with the supports, would affect the structure and performance of the catalysts [40–42]. Gálvez et al. [43] investigated activated carbons doped with some vanadium compounds including the ashes of a petroleum coke and applied them in $NH_3$-SCR. The surface acidity sites on activated carbon increased by doping with vanadium compounds, which was evidenced by $CO_2$-TPD. The amounts of $NH_3$ chemisorption of $V_2O_5$-loading samples were greater than the unloaded carbon sample. It was reported that NO conversion was above 40% at 125 °C and higher than 80% at 200 °C on the catalysts prepared with vanadium compounds, while unloaded sample only reached 43% at 200 °C.

Activated Carbon Fiber (ACF) has been widely applied as a catalyst support for removing the air pollutants due to its special characteristics. Metal oxide supported on ACF is an excellent candidate for low temperature $DeNO_x$ technology. Lu et al. [44] reported that $CeO_2$ supported on ACF provided 70% NO conversion at 150 °C, which is comparable to the vanadium loaded carbon-based catalyst [45].

Monolithic catalysts supported by carbon were also studied by some researchers. Assisted methods, such as microwaves [46], were used to scatter active components. Valdés-Solís et al. [47,48] produced AC/C (activated carbon/ceramic) monolithic catalyst support, and then vanadium and manganese active components were loaded by impregnation method. The results showed that catalytic performance was better than other similar catalysts above 125 °C, and kinetic constants of kinetic test were also better than those reported in literature before. Tang et al. [49] applied ultrasonic to enhance the loading and dispersion of active components in producing AC/C monolithic catalyst. The results showed that the amount of $MnO_x$ loading on AC/C support was greatly enhanced with ultrasonic.

Activated carbon has also been used as support for noble metal catalyst, aiming at improving low temperature performance in sulfur containing flue gas. An et al. [50] prepared a series of Pt/FC (fluorinated activated carbon) ceramic disc catalysts. Over 90% NO conversion was reached within 170–210 °C, and at the same time reductant can be completely transformed over Pt/FC/C catalyst. Moreover, such a catalyst has excellent water-resistant performance; the conversion of NO has no obvious change when 4% $H_2O$ existed in the reaction gas.

In general, Mn-based catalyst can be classified into three categories. The first type is non-supported $MnO_x$ catalysts, which means that from some precursors it can easily gain oxide catalyst containing Mn. The second type is Mn-based composite oxide catalysts. With the synergistic effect of two kinds of metal, it can get better low-temperature activity. The third type is Mn supported on various materials, such as $MnO_x/Al_2O_3$, $MnO_x/TiO_2$, and $MnO_x$/activated carbon. Table 1 summarizes the temperature ranges and activities of the three types of catalysts with Mn.

### 2.4. *Zeolite catalysts*

Among the new emerging SCR catalytic systems for mobile applications, many efforts are focused on metal promoted zeolites, which had been already proposed in the past for $NO_x$ abatement in stationary installations as well. Many ion exchanged zeolites were reported to be active in $NH_3$-SCR reaction, such as Fe [8,52], Cu [53,54], Mn [55], and Ce [56,57]. Among such a wide family of catalysts, iron and copper zeolites seem to be particularly interesting and have been extensively studied.

Rahkamaa-Tolonen et al. [7] reported that the zeolite-based catalysts were very promising for the ammonia SCR reaction. Especially, the activities at low and high temperatures were higher than the activities of commercial vanadia-based catalysts. From the studied catalysts, Fe-beta was active over a wide temperature range and had the lowest ammonia slip (the concentration of $NH_3$ after the catalyst) among the fresh catalysts, which were also supported by Liu et al. [58]. Choi et al. [59] reported that the low temperature activity of mordenite catalysts was obviously promoted by copper. Copper ions on the mordenite catalyst offered additional adsorption sites for NO and $NH_3$ which benefited NO reduction. They found that both the SCR activity and the adsorption capacities for NO and $NH_3$, including Brönsted acidity would increase with increasing proton and copper content of the catalysts. For a comprehensive understanding of Fe and Cu-based zeolite catalysts, Ford Company [60] studied the long term hydrothermal stability of base metal zeolite SCR catalysts for automotive applications as compared to a catalyst containing vanadia supported on titania that is typically used for $NO_x$ control on stationary sources world-wide and on heavy truck in Europe. After aging for 64 h at 670 °C to represent ~120k mi on a diesel vehicle with a regenerating soot filter, it was obvious that vanadia-based SCR was not an option for U.S. applications, and Fe and Cu–zeolite catalysts were optimal choice (Fig. 4). It could be seen that both of Fe/zeolite and Cu/zeolite have good thermal stability, but Fe/zeolite showed lower reactivity at low temperature than that of Cu/zeolite.

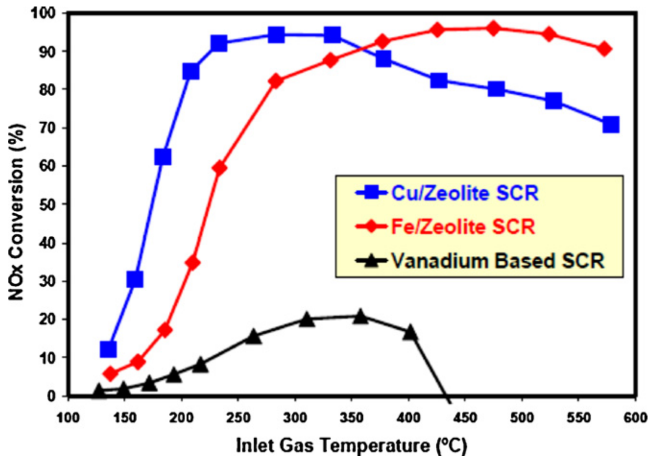

**Fig. 4.** $NO_x$ conversion over Cu, Fe, and vanadium based SCR formulations as a function of temperature. Reaction conditions: 30k $h^{-1}$, a round sample core of 1 in. diameter was taken from a washcoated monolith obtained from a supplier, 350 ppm NO, 350 ppm $NH_3$, 14.0% $O_2$, 5% $H_2O$, 5% $CO_2$, and $N_2$ balance, GHSV = 30,000 $h^{-1}$ [60].

Several methods, including impregnation method (IM), conventional aqueous ion-exchange (CA), improved aqueous ion-exchange (IA), solid state ion-exchange (SS), and chemical vapor ion-exchange (CV) [61–64], were reported to prepare zeolite catalysts for $NH_3$-SCR reaction, and tried to find a zeolite catalyst that has higher catalytic activities for $NH_3$-SCR compared to other known catalysts. Iron zeolite catalysts had demonstrated high $DeNO_x$ efficiency, and this was particularly true when iron was introduced by $FeCl_3$ sublimation [52]. According to several studies this preparation method resulted in the stability of catalyst for $NH_3$-SCR of NO in the presence of $H_2O$ and $SO_2$ [8,52]. Some researchers [62] supposed that Fe–ZSM-5 prepared by improved aqueous ion-exchange (IA) and conventional aqueous ion-exchange (CA) showed the highest activities for SCR of NO with ammonia, but some researchers proposed chemical vapor ion-exchange (CV) was the most effective technique. The main difference might be ascribed to the different contents of active species of Fe/zeolite catalysts under different experimental conditions.

## 3. Effect of reaction conditions

### 3.1. *Effect of $H_2O$ and $SO_2$*

Water vapor contributes to partially “destroy” acid sites acting to decrease the number of available active sites. Even in dry conditions, water should cover some active sites of the catalyst since it is produced by the SCR reaction. Co-adsorption with water is thus an important factor to consider in the description of the catalytic process [65,66]. Water always causes a certain extent of decrease in activity, no matter non-support metal oxide catalysts [22,31] or carbon based catalysts [43]. The effect of $H_2O$ can be divided into two results, reversible and unreversible. Reversible deactivation is brought on by $H_2O$ adsorption competed with $NH_3$ and NO. This effect will disappear when $H_2O$ is removed. Hydroxyl created by $H_2O$ chemisorption and decomposition on the surface of the catalysts will result in unreversible deactivation of the catalysts. Hydroxyl will only be pulled off under the temperature of 525–775 K, so this kind of deactivation cannot be removed by cutting of $H_2O$ in the gas. It was reported that the SCR activity on

**Table 1**
Research results on three kinds of Mn-based catalysts in literatures.

| Catalysts | Preparation methods (calcination temperature) | Reaction conditions | Highest $NO_x$ conversion/$N_2$ selectivity (temperature range) | Sources |
|---|---|---|---|---|
| **Non-supported $MnO_x$** | | | | |
| $MnO_x$ | Co-precipitation (100 °C) | 0.05%$NH_3$, 0.05%NO, 3%$O_2$ | 100% (100–150 °C) | [15] |
| $MnO_x$ | Precipitation (350 °C) | 0.05%$NH_3$, 0.05%NO, 5%$O_2$, 50,000 $h^{-1}$ | 100%/>82% (100–150 °C) | [16,17] |
| $MnO_2$ | Calcination (400 °C) | 0.055%$NH_3$, 0.055%NO, 2%$O_2$ | 97%/55% (177 °C) | [18] |
| Manganese ore | – | 0.045%$NH_3$, 0.04%NO, 3%$O_2$, 20,000 $h^{-1}$ | 100% (150–250 °C) | [14] |
| **Mn-based composite oxides** | | | | |
| $MnO_x$–CuO | Co-precipitation (350 °C) | 0.05%$NH_3$, 0.05%NO, 5%$O_2$, 30 000 $h^{-1}$ | 100%(50–200 °C) | [21–23] |
| $MnO_x$–$FeO_x$ | Co-precipitation (500 °C) | 0.1%$NH_3$, 0.1%NO, 2%$O_2$, 15 000 $h^{-1}$ | 100% (120–180 °C) | [13] |
| $MnO_x$–$FeO_x$–$TiO_2$ | Co-precipitation (400 °C) | 0.05%$NH_3$, 0.05%NO, 5%$O_2$, 50,000 $h^{-1}$ | 100%/>90% (200–300 °C) | [26,27] |
| $MnO_x$–$CeO_2$ | Co-precipitation (650 °C) | 0.1%$NH_3$, 0.1%NO, 2%$O_2$, 42,000 $h^{-1}$ | 100% (120–150 °C) | [22,23] |
| $MnO_x$–$SnO_2$ | Redox co-precipitation (500 °C) | 0.05%$NH_3$, 0.05%NO, 3%$O_2$ | 100% (120–200 °C) | [24] |
| **Mn supported catalysts** | | | | |
| $MnO_x/Al_2O_3$ | Pore volume impregnation (500°) | 0.055%$NH_3$, 0.055%NO, 2%$O_2$, 58,000 $h^{-1}$ | 95%/>65%(150–250 °C) | [11] |
| $MnO_x/TiO_2$ | Impregnation (400 °C) | 0.04%$NH_3$, 0.04%NO, 2%$O_2$, 50,000 $h^{-1}$ | 95%/72% (170 °C) | [51] |
| $MnO_x/TiO_2$ | Impregnation (400 °C) | 0.05%$NH_3$, 0.05%NO, 3%$O_2$ | 100% (150–200 °C) | [33] |
| $MnO_x/TiO_2$ | Sol–gel (500 °C) | 0.1%$NH_3$, 0.1%NO, 3%$O_2$, 40,000 $h^{-1}$ | 100% (120–200 °C) | [35] |
| $MnO_x$–$CeO_2$–$Nb_2O_5$/cordierite | Co-precipitation (650 °C) | 0.2%$NH_3$, 0.1%NO, 10%$O_2$, 52,000 $h^{-1}$ | 80%/96% (200 °C) | [36] |
| $MnO_x$/AC/C | Impregnation (400 °C) | 0.055%$NH_3$, 0.05%NO, 3%$O_2$, 10,610 $h^{-1}$ | 95% (250 °C) | [49] |

catalysts under wet reaction conditions was strongly dependent on the type of reductant used [67].

For the actual diesel engine exhaust system, the $H_2O$ content generated from the combustion of diesel fuel with a high carbon number is distinctive in the gas stream, and the development of a hot spot in the catalytic converter from the sudden burning of locally collected particulate can be expected. Consequently, achieving hydrothermal stability of the catalyst is a critical issue in the commercial application of urea-SCR technology to the exhaust stream from diesel engines. In a "dry gas" stream, Cu–zeolite has sufficient activity for the SCR of $NO_x$. The performance will be affected significantly when water exists. It has been commonly observed that the deactivation of SCR activity over Cu–ZSM-5 catalyst is mainly due to the degradation of zeolite support and/or the formation of Cu-aluminate by dealumination, the decrease in active reaction sites by the transformation of $Cu^{2+}$ to CuO, the redistribution of the reaction sites through the migration of $Cu^{2+}$, or a combination of these mechanisms [68–70].

One thing we should pay attention in the reaction of low temperature SCR is that, $SO_2$ in the gas may result in deactivation of Mn catalysts to a different extent. Coverage of the active sites by metal sulfates and ammonium sulfates is considered as the main reason for the decrease in the SCR activity. Kijlstra et al. [29,71] considered the formation of $MnSO_4$ as the main reason for the deactivation of $MnO_x/Al_2O_3$ catalysts, as $MnSO_4$ decomposes only at 1293 °C, resulting in difficulty of catalyst regeneration. Non supported Mn oxides perform badly on resisting to $SO_2$ and $H_2O$. Tang et al. [72] found that after 0.1% $SO_2$ and 10% $H_2O$ were injected, $NO_x$ conversion dropped to about 70%. When the injections of $SO_2$ and $H_2O$ were off, $NO_x$ conversion rate restored to about 90%. The authors believed that competitive adsorption was the reason for the reduction of the activity. Qi et al. [22] prepared $MnO_x$–$CeO_2$ catalysts which showed excellent SCR performance with 100 ppm $SO_2$ and 2.5% $H_2O$ at 150 °C. The activity of NO conversion decreased by 15% on $MnO_x$–$CeO_2$ in the presence of $SO_2$ and $H_2O$ in 3 h, and this effect was reversible. After doping with Pr or Fe, there was nearly no restraint to NO conversion in the presence of $SO_2$ and $H_2O$. But after being coated on small cordierite monoliths, Casapu et al. [36] indicated that after exposing to 50 ppm $SO_2$ the sulfated species formed on $MnO_x$–$CeO_2$ was very stable and an irreversible damage of the surface catalytic centers for the oxidation of NO to $NO_2$ appeared. However, the resistance of $SO_2$ was increased by adding Fe, V to Mn-based monolithic catalysts, but the catalytic activity at low temperature would decrease [49].

For $V_2O_5$ loaded AC catalysts, the existence of $SO_2$ showed promoting effect at low temperatures [73]. When the $V_2O_5$ loading was lower than 5 wt%, the addition of 400 ppm $SO_2$ promoted the SCR activity at 250 °C over $V_2O_5$/AC. In the presence of $SO_2$, the deactivation of the 1 wt%$V_2O_5$/AC catalyst started in the beginning of the experiment at temperature below 180 °C, but above 180 °C the promoting effect of $SO_2$ could be maintained.

Huang et al. [74] and others studied the effect of $SO_2$ and $H_2O$ on catalytic performance over $V_2O_5$/AC, using industrial semi-coke treatment gaining AC support (Fig. 5). The results showed that the effect of water vapor on the activity was very small, and the suppression of $H_2O$ was due to competitive adsorption. However, the effect of $SO_2$ was positive; the NO conversion would increase from 60% to 92% with the addition of $SO_2$ and kept stable. It indicated that $SO_2$ transferred to $SO_4^{2-}$ on the surface of catalyst, which improved the acidity of catalyst surface and then enhanced adsorption capacity of $NH_3$. The co-existence of $H_2O$ and $SO_2$ resulted in the decrease of activity obviously. The inhibition effect was possibly caused by sulfate particle formed from $SO_2$ and $H_2O$. Sulfate particles accumulated continuously on the surface of catalyst in the reaction process, which led to blocking of the pores and covering the surface of catalysts.

It was reported the calcination temperature would influence the $SO_2$ oxidation activity of vanadium containing catalyst in high

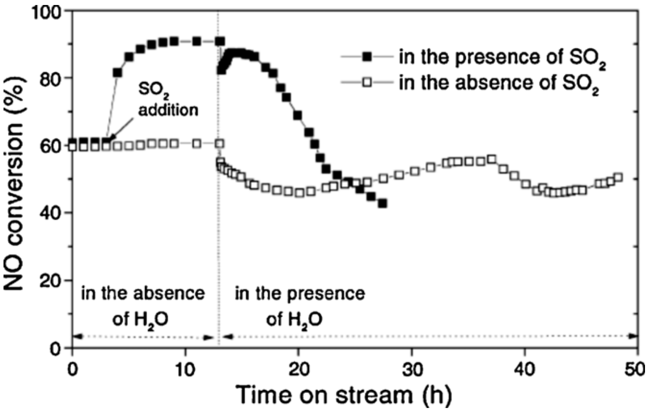

**Fig. 5.** The effect from $SO_2$ and $H_2O$ to $V_2O_5$/AC catalytic performance. Reaction conditions: 500 ppm NO, 600 ppm $NH_3$, 500 ppm $SO_2$, 3.4% $O_2$, 2.5% $H_2O$, Ar as balance gas, 90,000 $h^{-1}$, 250 °C [74].

temperature SCR reaction [75]. There is a possible way to improve $SO_2$ resistance by decreasing calcination temperature in preparing procedure, which would keep the low oxidation state of vanadium species. Ke et al. [76] prepared nano-$Co_3O_4$ by solid-state reaction at room temperature and investigated its $NH_3$-SCR performance in the presence of $SO_2$. After being sulfated in the presence of 500 ppm $SO_2$ and 3 vol.% $O_2$ at 300 °C for 48 h, bulk cobalt sulfate formed on the fresh $Co_3O_4$ sample. It was interesting that the activity under 250 °C of sulfated $Co_3O_4$ was improved compared with the fresh catalyst.

### *3.2. Effect of hydrocarbon*

During operation of diesel engines, the SCR catalyst is gradually deactivated by hydrothermal aging and catalyst poisoned by hydrocarbon coking. The deactivation of catalysts by aging and coking under evaluation conditions is also a disadvantage for their practical application. We studied that the catalytic activities for $NH_3$-SCR of $NO_x$ at 400 °C before and after 1000 ppm $C_3H_6$/He coking for 30 min over various catalysts, including iron exchanged H–ZSM-5, beta, mordenite, Y, ferrierite, and 4A zeolites. The results showed that Fe-MOR could keep high activity even after $C_3H_6$ coking, while the activities clearly decreased over other catalysts. This might be relevant to the zeolite structure. One dimensional large pore of MOR might be not favorable for hydrocarbon storage and coke formation compared to other zeolite catalysts [77]. In addition, we [78] have carefully investigated the effect of propene on the activity of Fe–ZSM-5 for $NH_3$-SCR, and proposed a deactivation mechanism of $Fe^{3+}$ active site blockage by propene residue. The NO conversion decreased in the presence of propene at various temperatures, while the effect was not significant when NO was replaced by $NO_2$ in the feed, especially at low temperatures (<300 °C). The blockage was mainly on $Fe^{3+}$ sites on which NO was to be oxidized to $NO_2$. Because of a little effect of HC on SCR activity of MOR, compositing catalyst of MOR and ZSM-5 may be one effective way to solve the HC poisoning.

## 4. The reaction mechanisms of $NH_3$-SCR at low temperature

### *4.1. Reaction pathway over metal oxide catalysts*

On the study of the mechanism, most researchers believe that $NH_3$ is adsorbed to Lewis acid center and intermediates like $NH_2$ [79–81] or adsorbed $NH_3$ [82–84] formed, then they react with aerial NO and $NO_2$ through E–R mechanism getting $N_2$ and $H_2O$. Kijlstra et al. [79,80] suggested that $Mn^{3+}$ location on the surface of $MnO_x/Al_2O_3$ was the Lewis acid center, and $NH_2$ on these sites can both react with aerial NO through E-R mechanism and react with activated nitrite intermediate adsorbed on the surface of the catalysts through L–H mechanism. $O_2$ was necessary in the formation of $NH_2$ and activated nitrite intermediate. $NH_4^+$ formed on Brönsted acid center did not participate in low temperature SCR reaction. The reaction scheme can be described as follows [79,80]:

$$O_2+2* \rightleftharpoons 2O-*$$

$$NH_3+* \rightleftharpoons NH_3-* \quad \text{Lewis acid } Mn^{3+} \text{ site}$$

$$NO + O-* \rightleftharpoons NO–O-* \quad \text{Bridged and monodentate nitrites}$$

$$NO–O-* + O-* \rightarrow NO_3-* + * \quad \text{Bidentate nitrate}$$

$$NH_3-* + O-* \rightarrow NH_2-* + OH-*$$

$$NH_2-* + NO \rightarrow N_2 + H_2O + * \quad \text{E–R mechanism}$$

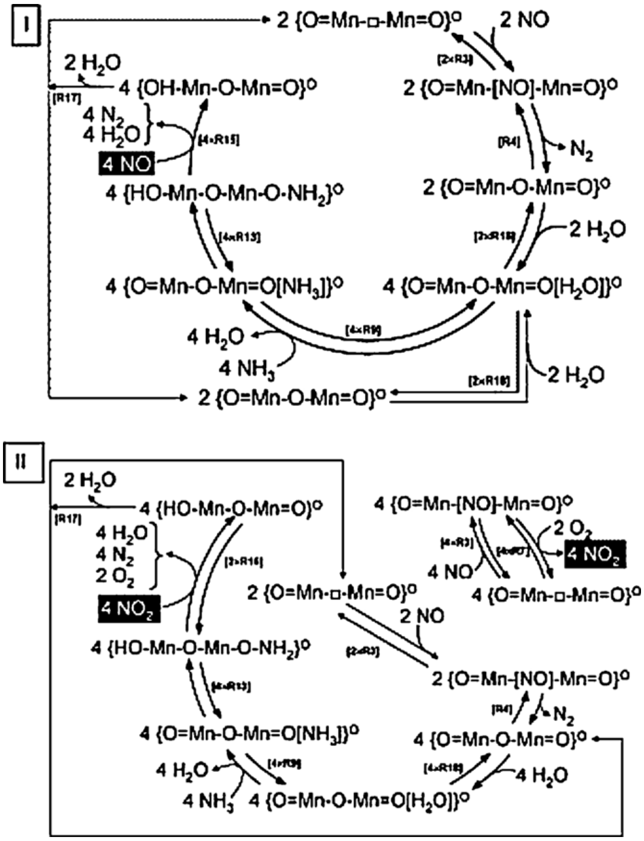

**Fig. 6.** Mechanism of the steady-state SCR reaction: (I) in the absence of oxygen; (II) in the presence of oxygen [82].

$$NH_2-* + NO–O-* \rightarrow N_2 + H_2O + O-* + * \quad \text{L–H mechanism}$$

$$2OH-* \rightleftharpoons H_2O + O-* + *$$

On the $MnO_x$–$CeO_2$ catalysts, mechanisms similar with that on the $MnO_x/Al_2O_3$ were pointed out by researchers. Qi et al. [22,81] proposed all the intermediates could transform into $NH_2NO$, which could further react to produce $N_2$ and $H_2O$. Similarly, Marban et al. [82] proposed an E-R mechanism over carbon-supported $Mn_3O_4$ catalyst, in which surface-active $NH_3$ species reacted with $NO_2$, and to a lesser extent NO, from the gas phase (see Fig. 6). It was reported that the selectivity of nitrous oxide increased with manganese loading and temperature, resulting in lower nitrogen selectivity. Doping with tungsten to the catalyst could increase the $N_2$ selectivity [11]. However, the $N_2$ selectivity still needs to be improved on Mn-based catalyst.

### *4.2. Mechanisms of Cu, Fe on zeolite catalysts*

The mechanisms of low temperature SCR on zeolite catalysts have been also investigated by researchers. Richter et al. [55] supposed symmetric O=N–O–N=O species formed on the $MnO_x$/NaY catalyst after contacting with NO. The results suggested a “diazotation” mechanism, in which $NH_3$ protonation to $NH_4^+$, NO interact with the catalyst and nitrite and nitrate surface species formed in the presence of $O_2$, followed by $NH_4^+$ reacting with $NO_2^-$ to produce $N_2$ and $H_2O$. However, a parallel “amide/nitrosamide” SCR reaction route was possible since prevailing Lewis acid sites on these catalysts should enable $NH_3$ activation via amide species.

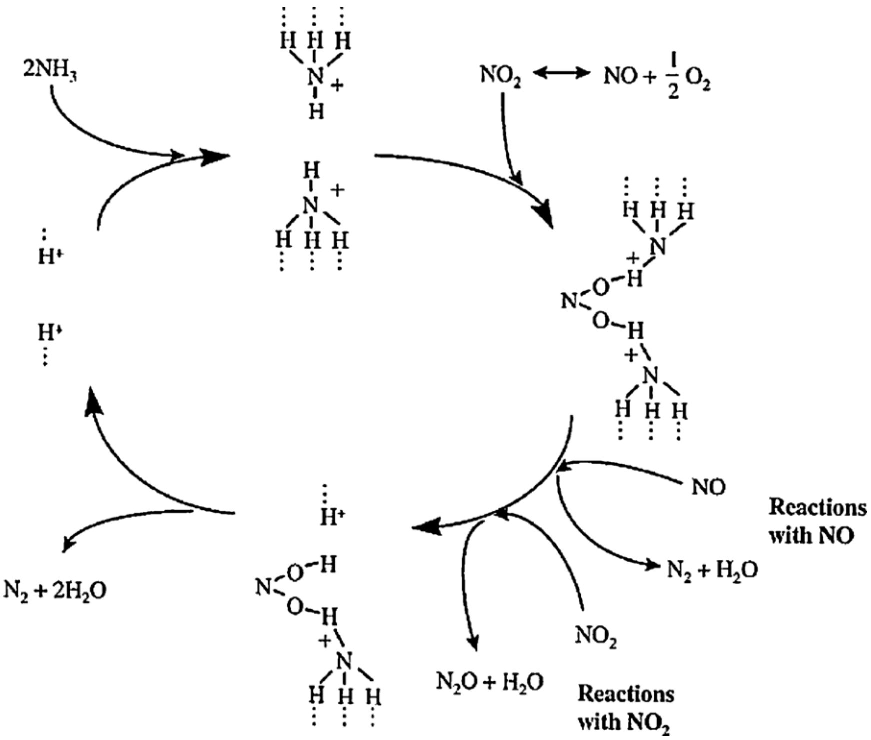

**Fig. 7.** Reaction mechanism of SCR of $NO_x$ with $NH_3$ over H-form zeolites [94,95].

Numerous studies have been conducted regarding the nature of Cu on the surface of zeolite, which is generally recognized as an active site for the present reaction system. It has been commonly accepted that isolated $Cu^{2+}$ and Cu–O–Cu dimer species on the catalyst surface play key roles in the $NH_3$-SCR reaction [85,86]. Paired $Cu^{2+}$ species, supposed by Komatsu et al. [87], were the active copper species in view of the relation between the specific activity and the copper concentration.

For Fe/zeolite catalysts, it is supposed that $Fe^{3+}$ ions with oxo-$Fe^{3+}$ sites [88], binuclear ions $[HO–Fe–O–Fe–OH]^{2+}$ [89] and some others were the active sites for the SCR reaction.

The results above contrasted with Schwidder [90,91], who prepared Fe–ZSM-5 catalysts by exchanging of Na–ZSM-5 with $Fe^{2+}$ ions formed by the dissolution of iron in acidic medium, and established that mononuclear Fe ions are active sites for both SCR reactions, but oligomers contribute as well. At the same time, oligomers (and aggregate surfaces) are more active in unselective oxidation of the reductant, which limits the temperature window of selective reduction of NO. Due to their higher oxidation potential, they cause undesired total oxidation of the reductant, particularly in the case of isobutane. Brandenberger et al. [92,93] supported and further developed these views, and determined Fe–O–Fe bridged and higher nuclear Fe-species are formed in a Fe–ZSM-5 sample, which may be calculated based on a simple Poisson distribution. They suggested that the SCR of NO by $NH_3$ is primarily caused by monomeric iron sites at temperatures below 300 °C.

A reaction mechanism which describes NO or $NO_2$ reduction by $NH_3$ over H-form zeolites was most developed and accepted (see Fig. 7) [94,95]. It suggested that adsorbed $NH_3$ is most reactive when it is bonded to the Brönsted acid sites in zeolites through three hydrogen bonds. An $NO_2$-type intermediate is formed on the zeolite surface during SCR reaction. Formation of this $NO_2$-type species appears to be a necessary step in the SCR reaction mechanism as the concentration of adsorbed NH3 does not decrease (i.e., react) until a band corresponding to this $NO_2$-type species appears.

In addition to the well-known “standard” SCR reaction, the so-called “fast” SCR reaction,

$$2NH_3 + NO + NO_2 \rightarrow 2N_2 + 3H_2O$$

plays a critical role at 180–300 °C in boosting the $DeNO_x$ activity of new generation urea-SCR converters for diesel vehicles integrated with an upstream preoxidation catalyst that partially oxidizes NO to $NO_2$ [96]. Grossale [97,98] present a systematic study of the chemical steps in the NO/$NO_2$-$NH_3$ fast SCR reaction over a commercial Fe–ZSM-5 catalyst (Fig. 8). Results show that the fast SCR reaction proceeds at low temperatures via a global sequence involving $NH_4NO_3$ or related surface species as intermediates, which is the same as that proposed previously for the fast SCR chemistry over V-based catalysts and other zeolite catalysts and thus is considered a general mechanism. It further showed that the redox reaction between NO and nitrates is the rate-controlling step and is inhibited by ammonia. Remarkably, the same strongly enhanced $DeNO_x$ activity observed in the fast SCR reaction also was observed in the absence of gaseous $NO_2$ but in the presence of surface nitrates. They accordingly propose a general summary of the fast SCR chemistry over V-based and zeolite catalysts that emphasize the key role of surface nitrates.

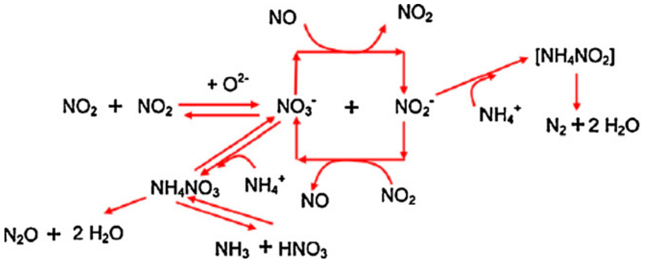

**Fig. 8.** Proposed reaction scheme for NO/$NO_2$-$NH_3$ SCR at low temperature [97,98].

## 5. Conclusions and perspective

The LTC is crucial in the removal of NO$_x$ from flue gas of power plant and exhaust gas of diesel engine at low temperatures. Much process on LTC has been made in the past decade, including the metal oxides, and metal exchanged zeolite catalysts. Manganese oxides are the most active components for NH$_3$-SCR of NO at low temperatures, and the activity of NO$_x$ reduction is correlated with the valence of manganese and phase structure of MnO$_x$. MnO$_2$ exhibited best catalytic activity in the temperature range of 100–300 °C, but its low N$_2$ selectivity required further improvement.

The resistance of H$_2$O and SO$_2$ on Mn based metal oxide is also a big challenge for its application at low temperatures. Efforts need to be made on detailed mechanisms of SO$_2$ poisoning and H$_2$O suppression effect at low temperatures. Synergistic effect of composite oxides is a hot topic in recent years. With the progress of analytical methods and analog computation, the synergistic effect among composite oxides, such as MnO$_x$ and other metal oxides is necessary, and a better understanding of the electronic interaction between SO$_2$, NO, NH$_3$ and catalysts is required, and a more comprehensive mechanism and kinetic model integrating the novel pieces of information provided by the experiments are undergoing.

Fe, Cu exchange zeolites, one kind of commercial catalysts for removal of NO$_x$ in diesel engine, have been extensively investigated recently, including activity, selectivity and thermal stability. Compared to the Fe/zeolite, Cu–zeolite has better activity at low temperature. Fe/beta shows great activity among all the Fe exchanged zeolite catalysts, however, the hydrocarbon coking is a problem for the application in diesel engine due to the incomplete combustion of fuel. It is also necessary to extend the window of temperature for Fe/zeolite catalysts at low temperature, while improve the activity for Cu/zeolite at high temperatures.

## Acknowledgements

This work was supported by National Natural Science Fund of China (Grant No. 51078203), National High Science & Technology Project (863, Grant No. 2009AA06Z301 and 2010AA065002) and Ford Motor Company.

## References

[1] P. Forzatti, L. Lietti, Heterogen. Chem. Rev. 3 (1996) 33.
[2] Y. Zhao, L. Duan, T. Larssen, L.H. Hu, J.M. Hao, Environ. Sci. Technol. 41 (2007) 1815.
[3] G. Busca, L. Lietti, G. Ramis, F. Berti, Appl. Catal. B: Environ. 18 (1998) 1.
[4] B.H. Engler, Chem. Ing. Tech. 63 (1991) 298.
[5] M. Devadas, O. Krocher, M. Elsener, A. Wokaun, N. Soger, M. Pfeifer, Y. Demel, L. Mussmann, Appl. Catal. B: Environ. 67 (2006) 187.
[6] J.P. Dunn, P.R. Koppula, H.G. Stenger, I.E. Wachs, Appl. Catal. B: Environ. 19 (1998) 103.
[7] K. Rahkamaa-Tolonen, T. Maunula, M. Lomma, M. Huuhtanen, R.L. Keiski, Catal. Today 100 (2005) 217.
[8] R.Q. Long, R.T. Yang, J. Am. Chem. Soc. 121 (1999) 5595.
[9] Z.M. Liu, S.I. Woo, Catal. Rev. 48 (2006) 43.
[10] Y. Hu, K. Griffiths, P.R. Norton, Surf. Sci. 603 (2009) 1740.
[11] L. Singoredjo, R. Korver, F. Kapteijn, J. Moulijn, Appl. Catal. B: Environ. 1 (1992) 297.
[12] B. Huang, R. Huang, D. Jin, D. Ye, Catal. Today 126 (2007) 279.
[13] R.Q. Long, R.T. Yang, R. Chang, Chem. Commun. (2002) 452.
[14] T.S. Park, S.K. Jeong, S.H. Hong, S.C. Hong, Ind. Eng. Chem. Res. 40 (2001) 4491.
[15] X.L. Tang, J.M. Hao, W.G. Xu, J.H. Li, Catal. Commun. 8 (2007) 329.
[16] M. Kang, E.D. Park, J.M. Kim, J.E. Yie, Appl. Catal. A: Gen. 327 (2007) 261.
[17] M. Kang, T.H. Yeon, E.D. Park, J.E. Yie, J.M. Kim, Catal. Lett. 106 (2006) 77.
[18] F. Kapteijn, L. Singoredjo, A. Andreini, J.A. Moulijn, Appl. Catal. B: Environ. 3 (1994) 173.
[19] X.F. Tang, J.H. Li, L.A. Sun, J.M. Hao, Appl. Catal. B: Environ. 99 (2010) 156.
[20] V.R. Galakhov, M. Demeter, S. Bartkowski, M. Neumann, N.A. Ovechkina, E.Z. Kurmaev, N.I. Logachevskaya, Y.M. Mukovskii, J. Mitchell, D.L. Ederer, Phys. Rev. B 65 (2002).
[21] M. Kang, E.D. Park, J.M. Kim, J.E. Yie, Catal. Today 111 (2006) 236.
[22] G.S. Qi, R.T. Yang, R. Chang, Appl. Catal. B: Environ. 51 (2004) 93.
[23] G. Qi, R. Yang, J. Catal. 217 (2003) 434.
[24] X. Tang, J. Li, L. Wei, J. Hao, Chinese J. Catal. 29 (2008) 531.
[25] F. Liu, H. He, C. Zhang, Chem. Commun. (2008) 2043.
[26] F. Liu, H. He, Y. Ding, C. Zhang, Appl. Catal. B: Environ. 93 (2009) 194.
[27] F.D. Liu, H. He, Catal. Today 153 (2010) 70.
[28] W.S. Kijlstra, J. Daamen, J.M. vandeGraaf, B. vanderLinden, E.K. Poels, A. Bliek, Appl. Catal. B: Environ. 7 (1996) 337.
[29] W.S. Kijlstra, M. Biervliet, E.K. Poels, A. Bliek, Appl. Catal. B: Environ. 16 (1998) 327.
[30] D. Pena, B. Uphade, E. Reddy, P. Smirniotis, J. Phys. Chem. B 108 (2004) 9927.
[31] R. Moreno-Tost, E.R. Castellon, A. Jimenez-Lopez, J. Mol. Catal. A: Chem. 248 (2006) 126.
[32] J.P. Chen, R.T. Yang, M.A. Buzanowski, J.E. Cichanowicz, Ind. Eng. Chem. Res. 29 (1990) 1431.
[33] J. Li, J. Chen, R. Ke, C. Luo, J. Hao, Catal. Commun. 8 (2007) 1896.
[34] J.A. Martin, M. Yates, P. Avila, S. Suarez, J. Blanco, Appl. Catal. B: Environ. 70 (2007) 330.
[35] Z.B. Wu, R.B. Jin, Y. Liu, H.Q. Wang, Catal. Commun. 9 (2008) 2217.
[36] M. Casapu, O. Krocher, M. Elsener, Appl. Catal. B: Environ. 88 (2009) 413.
[37] J.A. Sullivan, Catal. Lett. 79 (2002) 59.
[38] A.A. Nikolopoulos, E.S. Stergioula, E.A. Efthimiadis, I.A. Vasalos, Catal. Today 54 (1999) 439.
[39] P. Forzatti, Appl. Catal. A: Gen. 222 (2001) 221.
[40] T. Vergunst, M.J.G. Linders, F. Kapteijn, J.A. Moulijn, Catal. Rev. 43 (2001) 291.
[41] T. Vergunst, F. Kapteijn, J.A. Moulijn, Appl. Catal. A: Gen. 213 (2001) 179.
[42] S.B. Wang, G.Q. Lu, Carbon 36 (1998) 283.
[43] M.E. Gálvez, M.J. Lázaro, R. Moliner, Catal. Today 102–103 (2005) 142.
[44] P. Lu, C.T. Li, G.M. Zeng, L.J. He, D.L. Peng, H.F. Cui, S.H. Li, Y.B. Zhai, Appl. Catal. B: Environ. 96 (2010) 157.
[45] M.J. Lázaro, M.E. Gálveza, C. Ruiza, R. Juan, R. Moliner, Appl. Catal. B: Environ. 68 (2006) 130.
[46] M. Ouzzine, G.A. Cifredo, J.M. Gatica, S. Harti, T. Chafik, H. Vidal, Appl. Catal. A: Gen. 342 (2008) 150.
[47] T. Valdés-Solís, G. Marbán, A.B. Fuertes, Appl. Catal. B: Environ. 46 (2003) 261.
[48] T. Valdés-Solís, G. Marbán, A.B. Fuertes, Ind. Eng. Chem. Res. 43 (2004) 2349.
[49] X. Tang, J. Hao, H. Yi, J. Li, Catal. Today 126 (2007) 406.
[50] W. An, Q. Zhang, K.T. Chuang, A.R. Sanger, Ind. Eng. Chem. Res. 41 (2001) 27.
[51] P.G. Smirniotis, P.M. Sreekanth, D.A. Pena, R.G. Jenkins, Ind. Eng. Chem. Res. 45 (2006) 6436.
[52] A.Z. Ma, W. Grunert, Chem. Commun. (1999) 71.
[53] G. Centi, C. Nigro, S. Perathoner, G. Stella, Catal. Today 17 (1993) 159.
[54] J.H. Baik, S.D. Yim, I.S. Nam, Y.S. Mok, J.H. Lee, B.K. Cho, S.H. Oh, Top. Catal. 30/31 (2004) 37.
[55] M. Richter, A. Trunschke, U. Bentrup, K.W. Brzezinka, E. Schreier, M. Schneider, M.M. Pohl, R. Fricke, J. Catal. 206 (2002) 98.
[56] G. Carja, Y. Kameshima, K. Okada, C.D. Madhusoodana, Appl. Catal. B: Environ. 73 (2007) 60.
[57] E. Ito, R.J. Hultermans, P.M. Lugt, M.H.W. Burgers, M.S. Rigutto, H. van Bekkum, C.M. van den Bleek, Appl. Catal. B: Environ. 4 (1994) 95.
[58] Z. Liu, P.J. Millington, J.E. Bailie, R.R. Rajaram, J.A. Anderson, Micropor. Mesopor. Mater. 104 (2007) 159.
[59] E.Y. Choi, I.S. Nam, Y.G. Kim, J. Catal. 161 (1996) 597.
[60] G. Cavataio, J. Girard, J.E. Patterson, C. Montreuil, Y. Cheng, C.K. Lambert, SAE 2007-01-1575.
[61] G.S. Qi, R.T. Yang, Appl. Catal. B: Environ. 60 (2005) 13.
[62] R.Q. Long, R.T. Yang, Catal. Lett. 74 (2001) 201.
[63] G. Delahay, D. Valade, A. Guzman-Vargas, B. Coq, Appl. Catal. B: Environ. 55 (2005) 149.
[64] H.Y. Chen, W.M.H. Sachtler, Catal. Lett. 50 (1998) 125.
[65] M. Calatayud, B. Mguig, C. Minot, Surf. Sci. Rep. 55 (2004) 169.
[66] N. Apostolescu, B. Geiger, K. Hizbullah, M.T. Jan, S. Kureti, D. Reichert, F. Schott, W. Weisweiler, Appl. Catal. B: Environ. 62 (2006) 104.
[67] V.G. Komvokis, E.F. Iliopoulou, I.A. Vasalos, K.S. Triantafyllidis, C.L. Marshall, Appl. Catal. A: Gen. 325 (2007) 345.
[68] J.N. Armor, Catal. Today 26 (1995) 99.
[69] A.P. Walker, Catal. Today 26 (1995) 107.
[70] J.Y. Yan, G.D. Lei, W.M.H. Sachtler, H.H. Kung, J. Catal. 161 (1996) 43.
[71] W.S. Kijlstra, J.C.M.L. Daamen, J.M. vandeGraaf, B. vanderLinden, E.K. Poels, A. Bliek, Appl. Catal. B: Environ. 7 (1996) 337.
[72] X. Tang, J. Hao, W. Xu, J. Li, Chinese J. Catal. 27 (2006) 843.
[73] Z.P. Zhu, Z.Y. Liu, H.X. Niu, S.J. Liu, J. Catal. 187 (1999) 245.
[74] Z.G. Huang, Z.P. Zhu, Z.Y. Liu, Appl. Catal. B: Environ. 39 (2002) 361.
[75] a.M.H. Motonobu Kobayashi, Appl. Catal. B: Environ. 63 (2006) 104.
[76] R. Ke, J. Li, X. Liang, J. Hao, Catal. Commun. 8 (2007) 2096.
[77] A. Sultana, M. Haneda, T. Fujitani, H. Hamada, Micropor. Mesopor. Mater. 111 (2008) 488.
[78] J. Li, R. Zhu, Y. Cheng, C.K. Lambert, R.T. Yang, Environ. Sci. Technol. 44 (2010) 1799.
[79] W.S. Kijlstra, D.S. Brands, E.K. Poels, A. Bliek, J. Catal. 171 (1997) 208.
[80] W.S. Kijlstra, D.S. Brands, H.I. Smit, E.K. Poels, A. Bliek, J. Catal. 171 (1997) 219.
[81] G.S. Qi, R.T. Yang, J. Phys. Chem. B 108 (2004) 15738.
[82] G. Marban, T. Valdes-Solis, A. Fuertes, J. Catal. 226 (2004) 138.
[83] G. Marban, T. Valdes-Solis, A.B. Fuertes, Phys. Chem. Chem. Phys. 6 (2004) 453.
[84] F. Eigenmann, M. Maciejewski, A. Baiker, Appl. Catal. B: Environ. 62 (2006) 311.
[85] J.-H. Park, H.J. Park, J.H. Baik, I.-S. Nam, C.-H. Shin, J.-H. Lee, B.K. Cho, S.H. Oh, J. Catal. 240 (2006) 47.

[86] G. Centi, S. Perathoner, Appl. Catal. A: Gen. 132 (1995) 179.
[87] T. Komatsu, M. Nunokawa, I.S. Moon, T. Takahara, S. Namba, T. Yashima, J. Catal. 148 (1994) 427.
[88] M. Iwasaki, K. Yamazaki, K. Banno, H. Shinjoh, J. Catal. 260 (2008) 205.
[89] T.V. Voskoboinikov, H.Y. Chen, W.M.H. Sachtler, Appl. Catal. B: Environ. 19 (1998) 279.
[90] M. Schwidder, M.S. Kumar, K. Klementiev, M.M. Pohl, A. Bruckner, W. Grunert, J. Catal. 231 (2005) 314.
[91] M. Schwidder, W. Grunert, U. Bentrup, A. Bruckner, J. Catal. 239 (2006) 173.
[92] S. Brandenberger, O. Kröcher, A. Tissler, R. Althoff, Appl. Catal. A: Gen. 373 (2010) 168.
[93] S. Brandenberger, O. Krocher, A. Tissler, R. Althoff, Appl. Catal. B: Environ. 95 (2010) 348.
[94] J. Eng, C.H. Bartholomew, J. Catal. 171 (1997) 27.
[95] R.Q. Long, R.T. Yang, J. Catal. 207 (2002) 224.
[96] G. Madia, M. Koebel, M. Elsener, A. Wokaun, Ind. Eng. Chem. Res. 41 (2002) 3512.
[97] A. Grossale, I. Nova, E. Tronconi, D. Chatterjee, M. Weibel, J. Catal. 256 (2008) 312.
[98] A. Grossale, I. Nova, E. Tronconi, J. Catal. 265 (2009) 141.